

CONTROLLER PROTOTYPE DEVELOPMENT FOR DYNAMIC
POSITIONING SYSTEMS OF PLATFORMS

Decio Crisol Donha
Universidade de São Paulo-Depart^o. de Eng. Mecânica
05508 - São Paulo (SP) - BRAZIL

Hernani Luiz Brinati
Universidade de São Paulo-Depart^o. de Eng. Naval
05508 - São Paulo (SP) - BRAZIL

1990
Serviço de Bibliotecas
Biblioteca de Engenharia Mecânica, Naval e Oceânica

ABSTRACT

The development of a controller prototype used in the experimental part of a research involving Dynamic Positioning Systems (DPS) for semisubmersible platforms is presented.

The theoretical background and numerical implementation of the control system are briefly introduced. After that, the prototype construction is focused with special emphasis on the control software, that was fully developed by the authors, using two different approaches-applied to a linear stationary stochastic model. In both cases, using the separation principle, the control law is applied taking in consideration the estimate of the system state. The estimation is obtained by an adaptive filter based on the Kalman-Bucy procedure, incorporating a noise estimation algorithm and a dynamic compensation technique. The first control approach is based on the optimal control law (or LQG) and the other uses an adaptive method based on the existing duality between the estimator and the controller.

In order to evaluate the control system prototype performance a large number of dynamic positioning tests were conducted in the towing tank of Berlin Technical University. It was used a propelled aluminium model of a selected semisubmersible platform.

The analysis of trial results shows that the control system has a satisfactory performance being potentially useful in real conditions.

Keywords: DPS; dynamic positioning system; LQG control; optimal control; adaptive control; stochastic control; Kalman filter; control prototype; semisubmersible platform.

1. INTRODUCTION

Offshore exploration are expanding day by day to deeper and less accessible regions of the sea. In Brazil, where the largest part of oil production comes from the continental shelf, some exploration sites are under of a water depth of more than one thousand meters. Floating anchored and fixed conventional systems become economically unfeasible in such conditions. Anchored structures demand too much time for deployment and recovery of anchors and fixed types wait for solutions of complex technological problems. The dynamic positioning systems (DPS) is as a matter of fact the only real option in deep water applications, since tension legs platforms are still not more than a promise. However DPS, though its satisfactory technical performance, is still an expensive option.

The DPS is basically composed by three

subsystems: the measurement (sensors) system, which provides information about the vehicle position as well as environmental conditions; the logical unit (control system), which processes this information and evaluates the control actions; and the thruster system, usually a set of strategically distributed Kort-nozzle, azimuthal propellers, which produces the propulsion forces required to keep the vessel on station (Morgan, 1978). Looking for better performance, new researches in DPS are mainly centered on the first two subsystems. In this work only the control system is focused.

Next one presents an overview of the mathematical models used in the implementation of the control system software.

2. CONTROL SYSTEM DEVELOPMENT AND IMPLEMENTATION

Two alternative approaches were used to

develop the control software: an optimal control technique (LQG) and an adaptive one. In both cases, use is made of the separation principle, in such a way the control action is set up based upon the information supplied by an estimator. Figure 1 shows the scheme used for the control system implementation.

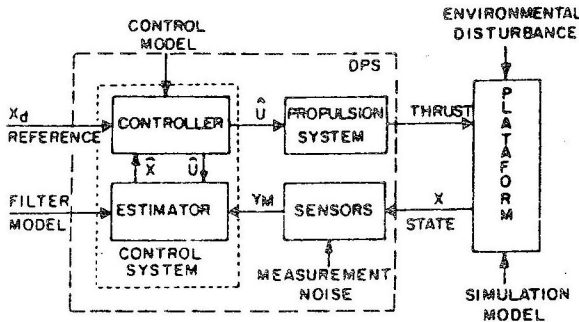


Fig.1: Control system scheme

In order to design the controller and the estimator the system is modelled as a linear stationary stochastic process:

$$\dot{X}(t) = FX(t) + G\omega(t) + LU(t) \quad (1)$$

where $X(\cdot)$ is the state vector; F is the plant matrix; G is the noise mixing matrix; $\omega(\cdot)$ is the dynamic noise vector; L is the input matrix and $U(\cdot)$ is the control vector.

Completing the model there is the measurement equation given by:

$$Y(t) = HX(t) + v(t) \quad (2)$$

where $Y(\cdot)$ is the observation vector; H is the output matrix and $v(\cdot)$ is the measurement noise vector; $v(\cdot)$ and $\omega(\cdot)$ are assumed to be uncorrelated zero mean gaussian white noise processes. The measurement noise properties are determined from the specific sensor characteristics, while the dynamic noise statistics are determined by an estimation algorithm similar to the Kalman filter technique.

2.1 State Estimation

The state estimation is obtained through an adaptive filter based on the Kalman-Bucy filter. It must be pointed out that the filter model was kept as simple as possible, aiming fast computations, since the procedure should be used in towing tank tests with a reduced scale model; in such conditions the time scale, with correspondent effects on data acquisition rates and thruster modulations, is reduced by a factor $\sqrt{\lambda}$, where λ is the scale factor between model and prototype. Nevertheless it is known, that a poor model representation may lead the filter to diverge (Jazwinski, 1970). To avoid filter divergence the Kalman-Bucy method

was modified introducing the dynamic model compensation technique and by the addition of an adaptive noise (Moro, 84; Rios Neto, 85). The first algorithm searches for a simple representation of environmental forces (wind, waves and currents), that were not directly represented in the model. The dynamic compensation is obtained extending the model state vector by the addition of a non modelled acceleration, modelled as a Gauss-Markov process and estimated altogether with the model state. The dynamic model covariance is evaluated step by step in such a way to minimize the measurement residue. The adaptive noise was introduced to take care on divergence caused by other factors like parameter uncertainty linearization and numerical errors, etc.

As usual in DPS analysis (Balchen, 1979; Grimble, 1980) the vehicle motion is assumed to be the linear superposition of high and low frequency motions. Low frequency motions are induced by wind, current and wave drift forces, while the high frequency part is due to the oscillatory components of wave and wind forces. Using that the filter mathematical model becomes:

$$\begin{bmatrix} \dot{X}_l(t) \\ \dot{X}_h(t) \end{bmatrix} = \begin{bmatrix} F_l & 0 \\ 0 & F_h \end{bmatrix} \begin{bmatrix} X_l(t) \\ X_h(t) \end{bmatrix} + \begin{bmatrix} G_l & 0 \\ 0 & G_h \end{bmatrix} \begin{bmatrix} \omega_l(t) \\ \omega_h(t) \end{bmatrix} + \begin{bmatrix} L \\ 0 \end{bmatrix} U(t) \quad (3)$$

$$Y(t) = [H_l \ H_h] [X_l(t) \ X_h(t)]^T + [v(t)] \quad (4)$$

where h and l indicate, respectively, the high and the low frequency motion variables or parameters.

The low frequency part of the model was derived from manoeuvring equations of the platform, where the added mass and damping coefficients were selected by an oriented search and from experimental results (Clauss, 1984). The high frequency part was modelled as a damped second order oscillator, including also an adaptive noise and the dynamic compensation technique, to get better performance in changing weather conditions. The used high frequency model is quite different from that proposed by Balchen (1979), who uses a non-linear high frequency model, leading the estimator to an extended Kalman filter.

The state vector for surge $X_1(\cdot)$ estimation, e.g., is:

$$X_1(t) = \begin{bmatrix} x_{l1}(t) & X_{l1}(t) & \epsilon_{l1}(t) \\ x_{h1}(t) & X_{h1}(t) & \epsilon_{h1}(t) \end{bmatrix}^T \quad (5)$$

where $\dot{x}_1(\cdot)$ are the surge velocities of the platform; $X_1(\cdot)$ are the platform displacements relative to the OX axis of a right hand oriented coordinate system, whose origin is fixed at the calm water surface over

the blow out preventer (BQP) valve, at the top of the well head. The OX axis grows to right; $\varepsilon_1(\cdot)$ are the non-modeled acceleration.

2.2 Controllers

It must be pointed out that in DPS only low frequency motions should be controlled, since the high frequency component leads to a zero mean averaged motion, due to its oscillatory characteristic. Any attempt to control high frequency motions will cause energy waste and wear and tear of equipments. Therefore the mathematical model for control purposes was obtained from the filter model using only its low frequency part; obviously it is omitted the non-modeled acceleration variable, since it is impossible to make a direct control of the environmental forces. Next, a brief presentation of the two approaches is made. Both were developed for linear stationary stochastic models, with structure similar to equations (1) and (2).

2.2.1 LQG Controller

In this case, the control law $U(\cdot)$ for equation (1) is determined by minimizing the following scalar quadratic performance index:

$$J = E \left(\frac{1}{2} \int_{t_0}^{t_f} X_c^T(t) V X_c(t) + U^T(t) P U(t) dt \right) \quad (6)$$

where E is the mathematical expectance operator; $V \geq 0$ and $P > 0$ are weighting matrices, whose elements are chosen in order to define the relative importance given to reduce the state deviation $X_c(\cdot)$ and the use of energy $U(\cdot)$ in the control process.

The optimal control solution for the linear stochastic problem is given by (Gelb, 1977):

$$\hat{U}(t) = -C(t) \hat{X}(t) \quad (7)$$

$$C(t) = P^{-1} L S(t) \quad (8)$$

$$\dot{S}(t) = -F^T S(t) - S(t) F - S(t) L P^{-1} L^T S(t) - V \quad (9)$$

$$S(t_f) = 0$$

where $C(\cdot)$ is the optimal control gain vector; $S(\cdot)$ is the solution of the Riccati matrix equation and $\hat{X}(\cdot)$ is the filter estimation for the control state vector:

$$X_c(t) = \begin{bmatrix} x_{b1}(t) & x_{b1}(t) \end{bmatrix}^T \quad (10)$$

The solution for the Riccati equation was obtained by a backward time integration of equation (9), where the values for V and P were established by an oriented search.

The optimal control gain vector $C(\cdot)$ is only function of the plant matrix and the weighting matrices V and P . Therefore, it can be calculated out of line, saving compu-

tational work and time.

2.3 Adaptive Controller

In the adaptive approach the control law $U(\cdot)$ is obtained using the existing duality between the estimator and the controller with and additional advantage in the present problem, developed for a stationary model, leading to a less complex solution than that proposed by Cruz (1985).

The resulting computation algorithm is fast enough to allow real time evaluation of the control variable.

To find the adaptive control law it is used a discret model, obtained from time discretization of equations (1) and (2) in a control interval, defined as the time lag between two modifications of $U(\cdot)$, also referred as the modulation interval of $U(\cdot)$.

The control action in a typical interval $(k, k+1)$ is calculated using the state estimate $\hat{X}(k)$ and the state vector error covariance $P(k)$, aiming to drive the state closer to the prescribed values. Formally, it is desired to satisfy the following relationship:

$$\phi[X_c(k+1)] = 0 \quad (11)$$

where $\phi[\cdot]$ is a vector of control functions and k is the present time.

In order to satisfy equation (11) it is used a reference state $X_r(k+1)$ obtained from the propagation of the last state estimation $X(k)$ with the control value of the previous interval, $U(k-1)$:

$$X_r(k+1) = \phi X_r(k) + \Omega U(k-1) \quad (12)$$

where ϕ is the transition matrix and Ω is the discret input vector (Gelb, 1979).

Considering the first-order variational equation associated with Taylor series expansion of equation (11) around $X_r(k+1)$, one obtains:

$$\phi[X_r(k+1)] + \phi^*(k+1) \delta X(k+1) + s(k+1) = 0 \quad (13)$$

where $s(\cdot)$ is the linearization error;

$$\phi^*(k+1) = \left. \frac{d\phi}{dX_c} \right|_{X_r(k+1)} \quad (14)$$

$$\delta X(k+1) = \phi \delta X(k) + \Omega \delta U + \Gamma \omega(k) \quad (15)$$

where Γ is the discretized noise mixing matrix and $\omega(k)$ is the white gaussian step function that replaces $\omega(t)$ assuming that the interval $(k, k+1)$ is arbitrarily small. Introducing the following definitions:

$$\delta X(k) \triangleq X_c(k) - X_r(k) \quad (16)$$

$$\delta U \triangleq U(k) - U(k-1) \quad (17)$$

into (15) and the obtained result into equa

tion (13), and by a proper choice of equation (11), one arrives to (Donha, 1989):

$$Z(k+1) = \Omega U(k) + \mu(k+1) \quad (18)$$

where

$$Z(k+1) \triangleq \Omega \hat{U}(k+1) - \phi [X_T(k+1)] \quad (19)$$

$$\mu(k+1) \triangleq \phi \delta X(k) + \Gamma \omega(k) + s(k+1) \quad (20)$$

The instantaneous value of $U(k)$ can be obtained from equation (18), since at the step k , $Z(k+1)$ and $s(k+1)$ are known and $\mu(k+1)$ is a white gaussian noise with the following properties:

$$\mu(k+1) = N[0, N(k+1)]$$

where $N(\cdot)$ is the covariance vector noise of $\mu(\cdot)$.

The estimated value $\hat{U}(k)$ for the control $U(k)$, that minimizes the root mean square of $[U(k) - \hat{U}(k)]$, assuming $U(k)$ to be unknown and statistically, independent from $\mu(\cdot)$ is given by (Cruz, 1985; Donha, 1989):

$$\hat{U}(k) = [\Omega^T N^{-1}(k+1) \Omega]^{-1} \Omega^T N^{-1}(k+1) Z(k+1) \quad (21)$$

3. CONTROL SYSTEM PROTOTYPE CONSTRUCTION

The control system prototype was built using the equipments shown in figure 2.

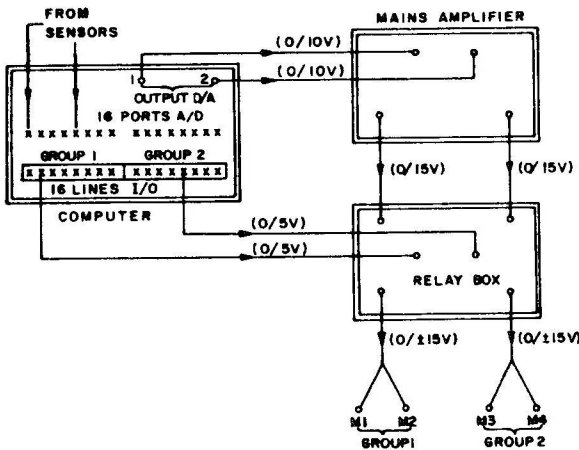


Fig.2: Control system hardware

The microcomputer, that supervises the other devices using the installed software, is the most important element of the prototype. It is used a portable PC/AT clone enhanced with an analog/digital interface board. The used computer has 640 kb memory capacity, a 80286 processor and a 80287 co-processor, working at 12Mhz clock frequency enabling it to perform a control cycle in the right scaled time, at least for model trials with only one degree of freedom. The

interface board is a 12 bits resolution device, with 16 analog (AD) input ports, 8 digital I/O lines and 2 analog (DA) output ports. The digital I/O lines may be configured only for input or only for output purposes and also transformed into 16 channels. These channels work in two independent groups, but each channel of a group works in the same way, i.e., when a group is active all its channels provide +5V output voltage signal. The interface board operation is controlled by a software package, composed of a set of subroutine libraries.

The propeller drive motors are designed to operate under till $\pm 15V$ in hazard conditions. When under negative tension the motor rotation is reversed, allowing thrust to be generated in the opposite direction.

Through board hardware modifications it is possible to obtain a maximum output tension in the analog ports of $\pm 10V$. A mains amplifier was then included in the control system hardware. Nevertheless, the available mains amplifier could only work under positive tensions. So, it was also necessary to include a set of relays between the amplifier and the motors. As it can be seen in figure 2, the relay box is monitored by the computer, through the I/O digital ports.

As it was mentioned before, the interface board is provided with only two analog output (DA) ports. In the model tests, when more than two propellers were used, it was necessary to link more than one motor to the same port, using parallel connections. Further on, the propulsion units (motor+propeller) have not equal performance, when working under the same voltage, consequently introducing undesirable moments on the model. To overcome this problem, the propulsion units are commanded, via software, to work under different voltages. The performance equalization software was developed using the results of previous trials of the propulsion units. These were captive model tests, leading to a precise relationship between motor input voltages and propeller output thrust.

Beside the control work, the microcomputer stores the trials results for later analysis.

4. TEST FACILITIES AND TRIAL PROGRAM

In the trials it was used an aluminium model of the RS-35 platform, shown in figure 3, built in a 1:53 scale, but not provided with the propulsion system specified for full scale trials.

The tests were carried out in the wave tank of Berlin Technical University with an available thruster system composed by three non-steerable, fixed pitch and speed variable propellers installed in Kort-nozzle. The thrust modulation was achieved by speed propeller variation through DC drive motors, directly assembled on the pro

PELLER shafts.

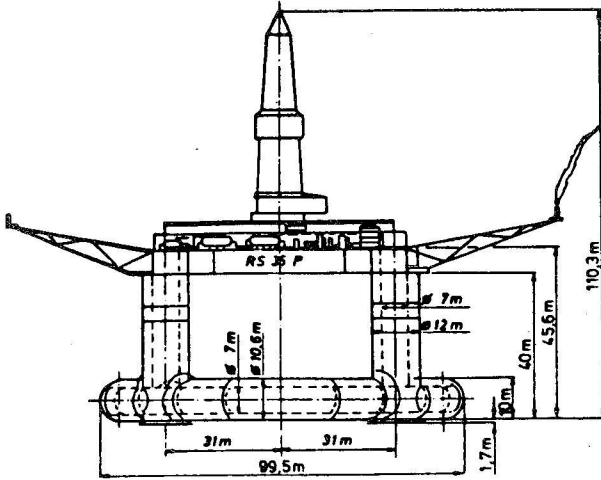


Fig.3: RS-35 platform

Towing tanks are not recommended to perform dynamic positioning tests since, in general, they are too narrow to allow larger sway motions of the model. Therefore, as a first step, it was decided to carry out the positioning test constraining the model sway and yaw motions and most of the results were obtained for pure surge motion.

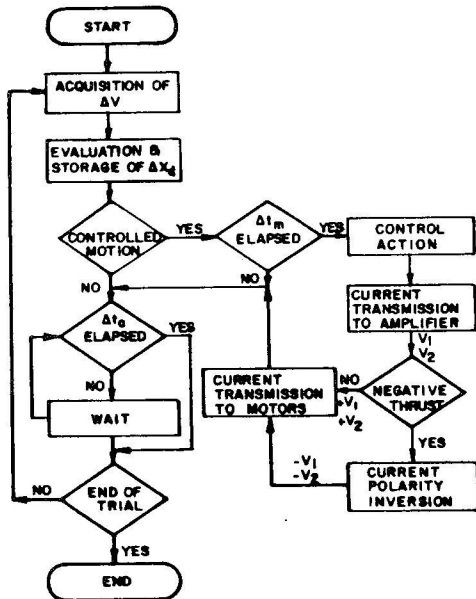


Fig.4: Control flow diagram

Referring to figure 2 and 4 a description of the control system prototype operation is now presented. Through one of the analog input ports (AD), at every regular interval Δt_a , the control prototype acquires the voltage ΔV generated by the

position sensor. Using the sensor calibration factor, that establishes the correspondence between ΔV and the model motion ΔX , a digital signal ΔX_d is generated by the control software. If another sensor is properly installed, it is possible to obtain the model attitude in the tank. For free model trials, when the propellers are not active, the prototype waits till Δt_a has been elapsed to make another acquisition and repeat the previous steps. In a controlled test, where the actuators are operating, after the information acquisition, the prototype checks out whether the modulation interval Δt_m has already elapsed ($\Delta t_m >> \Delta t_a$). If not, the end of Δt_a is verified again and the previous steps are repeated. If Δt_m is past, the prototype determines the thrust level to be applied and its distribution between the propulsion units, so that the model returns to the desired position and attitude. The level of the input motor tension is determined by the installed software in the following sequence: a) with the acquired informations (position and attitude) the Kalman filter estimates the state vector $\hat{X}(t)$, also stored for later analysis of filter performance; b) if the LQG control procedure is applied, using the previous established control gains and $\hat{X}_c(t)$, the necessary thrust level is on-line calculated. The thrust level signal is also stored for later analysis of controller performance; c) using the characteristic propeller curves, the input motor voltages for propulsion groups 1 (V_1) and 2 (V_2) are determined, in such a way to make the propellers work with the same load; d) if negative thrust must be produced and propellers reversed, the current polarity already amplified is inverted by a prototype order, that switch on a specific relay, through one of the I/O digital lines of the board; e) the amplified currents with proper polarity feed then the drive motors. Next the prototype checks out whether a new Δt_a has already elapsed, starting another control cycle.

A control cycle takes 0.08s for each degree of freedom. In full scale applications the acquisition interval Δt_a is set around 1.0s, to avoid filter divergence. For large platforms, like the RS-35, the modulation time interval Δt_m of propeller is set around 21.0s, to reduce wear and tear of propulsion system. In the trials, using the selected RS-35 model, Δt_a and Δt_m are reduced respectively, to 0.137s and 2.88s. So it is impossible to control more than one degree of freedom in the right scaled time using this computer.

5. RESULTS

When the propulsion system operates under the DPS supervision, one has a controlled condition test. These tests were carried out only under irregular wave excitation, but generated from different wave spectra. The model trials included wave

trains with significant wave height varying between 2.0 and 9.0m generated from Pierson-Moskowitz and Jonswap spectra. Since the wave excitation arised from Jonswap spectrum is more rigorous, only controlled tests under these waves are presented here. Other trials results can be found in Donha (1989a;b; 1990).

The trial program enclosed controller performance tests with both the LQG and the adaptive algorithm. In order to make easy the comparison, all the tests results are presented in full scale.

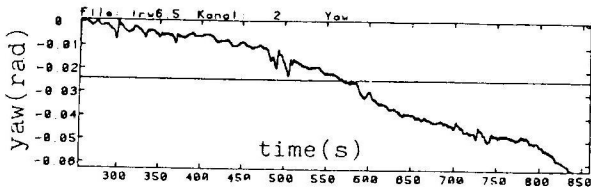


Fig.5a: Free condition-Yaw

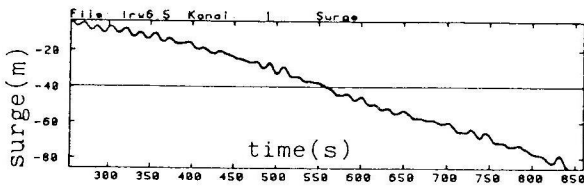


Fig.5b: Surge displacement

Figures 5a-b show a typical free condition test, when the model has 6 degree of freedom, drifting under wave excitation. Figure 5a presents the model yawing in radians, showing that in a test of 840s the platform changes its attitude of about 0.06 rad (3.5°), which is considered a small angular displacement. This behaviour was expected due to the platform simmetry and the excitation conditions; in other tests similar results were observed. As it is shown in figure 5b the platform drifted 85.0m along this test, which gives a surge drift velocity of 0.10 m/s.

A typical controlled test lasted 250s, corresponding to a 30 min full scale trial. To evaluate the controller robustness, when a very different excitation shows up, the wave generator was set to work only in the first 200s. After that the excitation is only due to the reflected waves.

Figure 6a-c present test results obtained with the model controlled by the LQG algorithm, using three propellers to control the surge motion. In figura 6a the lighth line represents the state estimation given by the filter and the heavy line the displacement performed by the platform (measured motion). One sees that the filter matches the state very well and that the platform presented maximum excursions of 42.0m at 840s and 1350s, but, despite the hazardous condition, the platform returns to the desired position, indicated by the zero line in this graphic.

Figure 6b shows the filter velocity es-

timations; the light line represents the low frequency velocity, whilst the heavy line corresponds to the total velocity (low plus high frequency components). This graphic shows that the filter separates fairly well the two components sending to the controller a very smooth low frequency signal.

Figure 6c presents the amount of propeller thrust used during this test. Some violent responses are probably due to an excessive cost penalty imposed on the velocity state. In spite of that the thrust level is reasonable, considering the excitation magnitude.

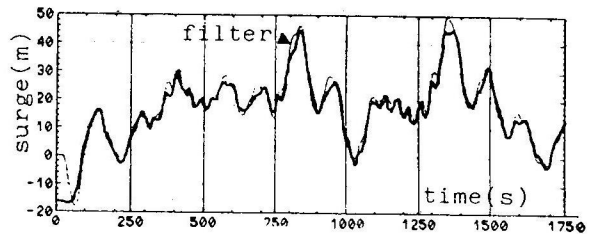


Fig.6a: Surge displacement-LQG

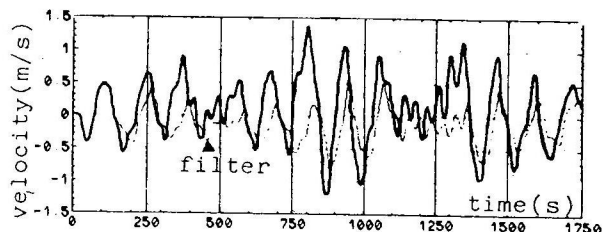


Fig.6b: Surge velocity - LQG

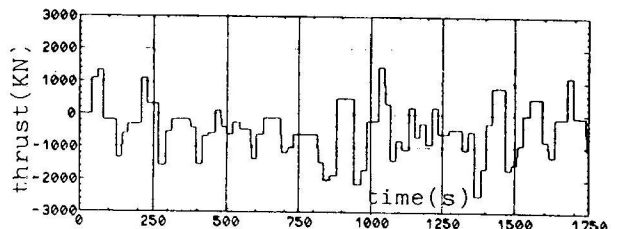


Fig.6c: Thrust level-LQG control

A model trial with the same wave excitation described above was carried out with the platform controlled by the adaptive algorithm. The results are shown in figure 7a-b; it may be seen from figure 7a that the filter (light line) matches the state very well too, and that the maximum platform deviation is 36.0m at 1750s, which is less than that achieved in the previous test. In figure 7b it is presented the time series of the generated thrust. Comparing to the time series shown in 6c, this is a very smoothed one. As a matter of fact, similar results were obtained in all other tests, leading to the conclusion that the adaptive algorithm has a better performance than the LQG one, since less energy is used to achieve basically the same deviation from the desired position.

Another point still under investigat-

ions is the considerable displacement offset observed in the tests, as shown in figures 6a and 7a, specially considering that the propulsion system was not saturated in any test, meaning that energy for control purposes is still available. Regarding to the results obtained in several digital simulations, where the referred offset did not occur, a probable explanation hypothesis is that the sensors used in the model trials were generating measurements with a systematic error.

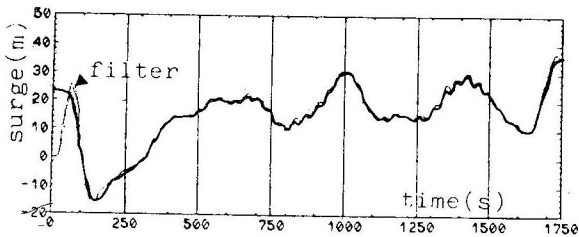


Fig.7a: Surge displacement-Adapt.

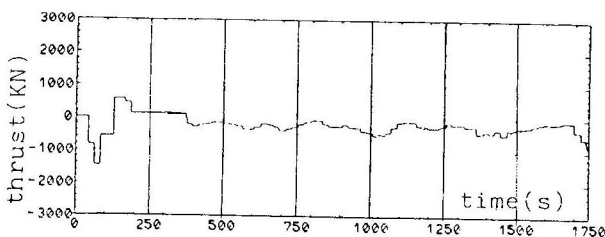


Fig.7b: Thrust Level-Adaptive Control

6. CONCLUSIONS

A controller prototype for the dynamic positioning system of a semisubmersible platform has been successfully developed and tested under several weather conditions. Its performance was considered satisfactory, even without using a proper thruster system. The utilization of the dynamic model compensation technique and the introduction of an adaptive noise, modifying the Kalman-Bucy filter allowed the development of an estimator with a very good performance, preventing divergence and giving close estimation of the non-modelled effects.

The implemented adaptive control law, formulated as the solution of a sequential parameter estimation problem, seems to offer a greater potential of employment in real applications than the LQG one. It is important to point out that the capability of good estimations for the state variables as well as the non-modelled accelerations was crucial for the good performance of the adaptive controller.

Computational performed simulations show that the observed displacement offsets could be eliminated.

The quality of the results obtained in the trial program gives a measure of the feasibility for full scale implementation of the proposed control system. To achieve

conclusive answers, one should still investigate (a) the effects of other types of perturbation—such as wind and currents; (b) the influence of a concomitant control of all horizontal motions of the vehicle; (c) the robustness of the controller under extreme situations; (d) at last the quality of results under full scale trials. Despite that, a good performance in other situations may be expected due to the inherent characteristic of the proposed estimator to deal with state noise and its capability for model compensation.

7. REFERENCES

- BALCHEN, J.G. & Allii, (1979). "A Dynamic Positioning System Based on Kalman Filtering and Optimal Control". Modeling, Identification and Control, University of Trondheim, Norway.
- CLAUSS, G.F., (1989). "Stability and Dynamics of Semisubmersible After Accidental Damage". OTC (4729) pp:159-164, Houston, Texas.
- CRUZ, J.J. & RIOS-NETO, A. (1985). "A Stochastic Rudder Control Law for Ship Path-following Autopilots". Automática, Vol. 21, nº 4, pp:371-384, Pergamon Press Ltda, 1985, England.
- DONHA, D.C., (1989a). "Estudo, Implementação, Teste e Avaliação de um Sistema de Posicionamento Dinâmico". São Paulo, University of São Paulo, PhD thesis, 396 pp.
- DONHA, D.C. & BRINATI, H.L., (1989b). "Towing Tank Test of a Dynamic Positioning System". Brazil Offshore, 89, Rio de Janeiro, 15 pp.
- DONHA, D.C. & BRINATI, H.L., (1990). "Control System Prototype for Dynamic Positioning System of Semisubmersible". OTC (6257), Houston, Texas.
- GELB, A. & Allii. (1974). "Applied Optimal Estimation". Cambridge, MIT Press.
- GRIMBLE, J.J. & Allii, (1980). "The Design of Dynamic Ship Positioning Control Systems Using Stochastic Optimal Control Theory". Optimal Control Applications & Methods, Vol. 1, pp:167-202, 1980, John Wiley & Sons Ltda, England.
- JAZWINSKI, A.H. (1970). "Stochastic Processes and Filtering Theory". New York, Academic Press.
- MORGAN, A.C. (1978). "Dynamic Positioning Offshore Vessels". The Petroleum Publishing Co., Oklahoma.
- MORO, J. & BRINATI, H.L. & RIOS-NETO, A. (1984). "Um Controlador Adaptativo de Atitude para Satélites Artificiais Terrestres". 5º Congresso Brasileiro de Automática, pp:838-843, Campina Grande, 1984.
- RIOS-NETO, A. & KUGA, H.K. (1985). "Kalman Filtering State Noise Adaptive Estimation". Telecommunication and Control, pp:210-213, J.A.M.F. de Souza Editor, TELECON'1985, Rio de Janeiro.